Evidence of deuterium excess in water vapor as an indicator of ocean surface conditions

Ryu Uemura,[1,2] Yohei Matsui,[3,4] Kei Yoshimura,[5] Hideaki Motoyama,[1] and Naohiro Yoshida[3]

[1] Stable isotopes of water are important climatic tracers used to understand atmospheric moisture cycling and to reconstruct paleoclimate. The combined use of hydrogen and oxygen isotopes in water provides an additional parameter, deuterium excess (*d*), which might reflect ocean surface conditions in moisture source regions for precipitation. The *d* records from polar ice cores covering glacial-interglacial cycles were used to reconstruct ocean surface temperatures at the moisture source, enabling elimination of source effects from the conventional isotope thermometer. However, observations of the essential relationship between *d* in vapor and ocean surface conditions are very limited. To date, theoretical values predicted using simple and atmospheric general circulation models (GCM) have not been validated against the data. Here, we show the isotope ratios of atmospheric water vapor near the ocean surface in middle and high latitudes of the Southern Ocean. Our observations show that *d* negatively correlates with relative humidity (*h*) above the ocean and correlates with sea surface temperature (SST). Despite the fact that the GCMs would underestimate the absolute value of observed *d*, the observations and simulation results are consistent for slopes between *d* versus *h* and *d* versus SST, suggesting that *d* is a reliable index to *h* and SST over the ocean surface.

1. Introduction

[2] The stable isotope ratios of hydrogen (D/H) and oxygen ($^{18}O/^{16}O$) in water reflect various exchanges between water phases through the global water cycle. These isotope ratios are important climatic tracers used to understand atmospheric moisture cycling [*Worden et al.*, 2007; *Yamanaka and Shimizu*, 2007; *Noone*, 2008] and to reconstruct paleoclimate from ice cores [*EPICA Community Members*, 2004; *Kawamura et al.*, 2007]. The relative abundance of the heavy isotopes, $HD^{16}O$ and $H_2^{18}O$, is represented by the delta value, $\delta = (R_{sa}/R_{VSMOW} - 1)$, where R_{sa} is the isotope ratio of sample and R_{VSMOW} is the isotope ratio of the Vienna Standard Mean Ocean Water (VSMOW). Past air temperatures can be inferred by either δD or $\delta^{18}O$ in the ice core because the equilibrium fractionation between vapor and condensate is temperature-dependent. In addition, the precipitation moisture source information can be derived from the deuterium excess ($d = \delta D - 8 \times \delta^{18}O$) parameter, which mainly reflects the kinetic fractionation process, such as evaporation from the ocean into the atmosphere [*Dansgaard*, 1964].

[3] Evaporation, as the first step in the hydrological cycle, plays a key role in determining relation between δD and $\delta^{18}O$ in global precipitation and snow. A Craig-Gordon type simple evaporation model [*Craig and Gordon*, 1965; *He and Smith*, 1999] describes the initial isotope content in the water vapor (δ_{v0}) as a function of the isotope contents of the evaporating water (δ_E), deuterium excess (*d*), relative humidity (*h*), and sea surface temperature (SST). Note that relative humidity is defined as a value normalized on the SST (*h**) in the model. The value of *h** can be approximated to *h* near the ocean surface because the SST is almost equivalent to the air temperature.

[4] However, the value of δ_{v0} is not estimated easily because it is difficult to estimate or observe the δ_E. Making a global-scale closure assumption ($\delta_{v0} = \delta_E$) [*Merlivat and Jouzel*, 1979], the model can be written as

$$1 + \delta_{V0} = \frac{1}{\alpha} \frac{(1-k)}{1-kh} (1 + \delta_{\text{ocean}}), \qquad (1)$$

where *k* is a kinetic fractionation factor, α is an equilibrium fractionation factor, and δ_{ocean} is an ocean isotope composition. In principle, the *d* versus *h* correlation arises because the magnitude of the kinetic effect (i.e., moisture

[1]National Institute of Polar Research, Research Organization of Information and Systems, Tokyo, Japan.

[2]Now at Laboratoire des Sciences du Climat et l'Environnement, CEA-CNRS, Gif-sur-Yvette, France.

[3]Department of Environmental Science and Technology, Tokyo Institute of Technology, Tokyo, Japan.

[4]Now at School of Earth Sciences, Ohio State University, Columbus, Ohio, USA.

[5]Climate Research Division, Scripps Institution of Oceanography, La Jolla, California, USA.
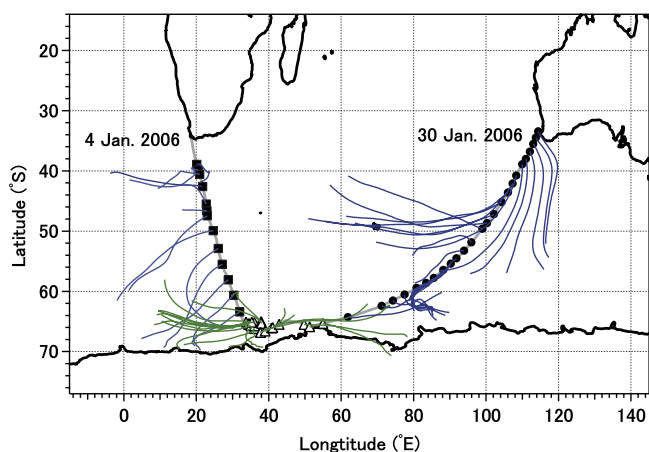
Figure 1. Sampling sites on a map of the ship route (gray) and 2 day backward trajectories (from 35 to 65°S shown by the blue line and south of 65°S shown by the green line) and each sampling site (solid squares, open triangles, and solid circles).

gradient between sea surface and overlying unsaturated vapor) governs molecular diffusive transport from the saturated layer to drier free air. On the other hand, the d is also controlled by the SST through the temperature dependence of α. This model predicts that d in marine vapor increases when relative humidity (h) decreases ($-0.43‰/\%$) and when the sea surface temperature (SST) increases ($0.35‰/°C$) [*Merlivat and Jouzel*, 1979]. Although this estimation is useful to understand underlying mechanism between d and ocean surface conditions, the global-scale closure assumption ($\delta_{v0} = \delta_E$) causes systematic bias [*Jouzel and Koster*, 1996]. A thorough method to predict the isotope ratios of marine vapor is to simulate the water cycle using an atmospheric general circulation models (GCMs) that accounts for complexity of hydrological processes [*Joussaume et al.*, 1984; *Jouzel et al.*, 1987; *Hoffmann et al.*, 1998; *Mathieu et al.*, 2002].

[5] The subsequent precipitation process, which is controlled by equilibrium fractionation, would exert a minor impact on the d parameter; thereby, changes in ocean surface conditions at the moisture source can be estimated from the d in polar precipitation. The d records from Antarctic ice cores show that significant ~41,000 year periodicity cycle over the glacial-interglacial cycles [*Vimeux et al.*, 1999; *Vimeux et al.*, 2001; *Uemura et al.*, 2004]. Because d depends on SST, h, and the wind speed at the vapor source region and on the supersaturation ratio where snow crystals form [*Jouzel and Merlivat*, 1984], several assumptions are necessary to interpret d in ice cores as an index of a single variable. The glacial-interglacial changes in d were interpreted as changes in relative humidity [*Jouzel et al.*, 1982] and temperatures at the moisture source ocean [*Cuffey and Vimeux*, 2001; *Stenni et al.*, 2001; *Vimeux et al.*, 2002]. In particular, information related to the moisture source temperature is valuable for accurate estimation of past air temperature changes at the site [*Cuffey and Vimeux*, 2001; *Masson-Delmotte et al.*, 2005].

[6] However, the interpretation of d in ice cores relies on the fact that various models, which range from simple Rayleigh-type models [*Jouzel and Merlivat*, 1984; *Johnsen*

et al., 1989; *Ciais and Jouzel*, 1994] to the isotopic general circulation model (GCM), predict a close relationship between d and ocean surface conditions. The crucial relationship between d, SST and h has not yet been validated against data related to the initial vapor because of scarce observations on d of vapor near the ocean surface and its physical conditions. A few in situ measurements of vapor isotopes in the oceans have been reported [*Craig and Gordon*, 1965; *Lawrence et al.*, 2004]; most of them specifically pertain to either δD or $\delta^{18}O$. In fact, d has not been observed except for subtropical oceans [*Craig and Gordon*, 1965] and the Mediterranean Sea [*Gat and Garmi*, 1970; *Gat et al.*, 2003]. To fill the data gap on the vapor isotope compositions in the Southern Ocean, we measured isotope compositions of air moisture using a mechanical cold trap on a ship over the South Indian Ocean and Southern Ocean, which is a part of main moisture source (30°S – 65°S ocean) for Antarctic precipitation [*Delaygue et al.*, 2000] (Figure 1). Our observations show that d negatively correlates with relative humidity (h) above the ocean and correlates with sea surface temperature (SST). We discuss the differences between the observation and simulation results from a couple of isotope GCMs; a rather conventional simulation forced only by surface boundary (SST and sea ice) [*Jouzel et al.*, 1987; *Delaygue et al.*, 2000] and a more realistic simulation in high time resolution from a newly developed isotope GCM with additional forcing of observed atmospheric thermodynamical fields [*Yoshimura et al.*, 2008].

2. Methods

2.1. Performance Test of Vapor Sampler

[7] Atmospheric vapor was sampled cryogenically using a specially designed glass flask for determination of isotope ratios. Since accurate and precise sampling of vapor is needed in order to investigate d parameter, we carefully developed a vapor sampling system and tested its performance. Figure 2 shows a glass-made water vapor sampler that is designed for widely ranged vapor concentrations. This trap is an adaptation of Horibe trap [*Horibe and*
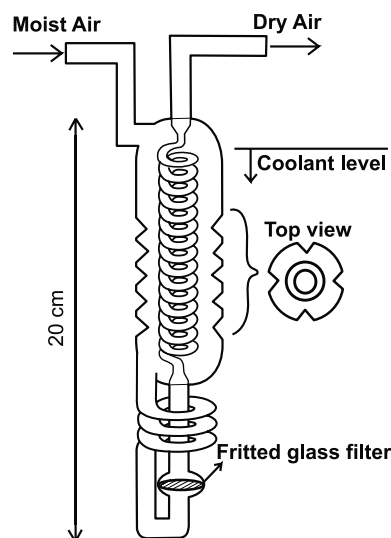

Figure 2. Schematic of glass made vapor trap.

Table 1. Efficiency Test for Vapor Trapping Apparatus

	Melted Iceberg		Distilled Sea Water	
	Trapped Vapor ($n = 5$)[a]	Injected Water ($n = 10$)[b]	Trapped Vapor ($n = 2$)[a]	Injected Water ($n = 4$)[b]
δD (‰)	-283.4 ± 0.5	-284.5 ± 0.3	-1.0 ± 0.9	-1.2 ± 0.2
δ^{18}O (‰)	-36.41 ± 0.04	-36.54 ± 0.02	-0.37 ± 0.08	-0.37 ± 0.0
d (‰)	7.8 ± 0.4	7.8	2.0 ± 1.6	1.8

[a]Average and standard deviation (1σ) of the replicated experiments (n indicates number of experiments).

[b]Average and standard deviation of the replicated experiments (n indicates number of measurements of water against VSMOW and Standard Light Antarctic Precipitation waters).

Takakuwa, 1973]. Residual vapor were sufficiently trapped by narrow and long glass tube, and a glass filter prevents outflow of trapped snow. The major modification is that spiral tube was inserted inside of wide end (∼45 mm OD) where the vapor is trapped efficiently with the surface of spiral tube cooled by the dry air. Further, the trap is compact enough to use onboard ship.

[8] The accuracy of the vapor sampling system had been tested carefully in the laboratory. The apparatus developed for the test comprises (1) a drying air unit, (2) a water injection port, and (3) a cold trap. All components were connected with a Teflon tube (fluorocarbon polymer, 3/8 inch) and Cajon and Swagelok (Swagelok Co., Ohio, USA) connections. First, the water vapor in the laboratory air was removed using a drying unit containing silica gel and a glass-made cold trap that was placed in a Dewar flask filled with liquid nitrogen. Second, the line led to a glass tube with a septum port from which water was injected. To enhance evaporation, a part of tubing was narrowed so that water bubbled within the tube. Then, the generated vapor was trapped cryogenically using a vapor trap in dry ice fluorinert bath with temperature maintained between −75 and −78°C (The flourinert is a liquid fluoric compound that has very low viscosity at low temperatures).

[9] After the tube and cold trap had been sufficiently dried by the dried air, 3.00 g of the water was injected into the septum. Humidity and temperature of the evolved moist air were monitored using a sensor situated within the line. Approximately 3 h after injection, all water was evaporated during which the relative humidity of moist air was changed from ∼95 to ∼0%. Both ends of cold trap were sealed immediately with Parafilm. The Parafilm was used to avoid

the risk of bursting of the glass trap from expansion of the air. After the trapped vapor (ice and snow) was melted, the ends were plugged immediately with silicon stoppers. The weight of the cold trap was measured before and after the collection; the calculated weight recovery was 100 ± 0.01%, suggesting that the fraction of lost vapor is very small. Two water samples, a melted iceberg and distilled seawater, were used for the test; the results are presented in Table 1. Deviations between the sampled and known waters were 1‰ for δD and 0.05‰ for δ^{18}O. Although the isotope ratios of the collected vapor were slightly heavier than those of the original waters, these values are mutually indistinguishable in 2-sigma of analytical error.

2.2. Ship Observation and Isotope Analysis

[10] Observations were conducted between 30 December 2005 to 30 January 2006 along the route linking Cape Town, Lützow-Holm Bay, and Fremantle onboard the Tokyo Kaiyou Daigaku *R/V* Umitaka-maru during the 18th Cruise (Figure 1). Isotopic sampling was done 2–3 times per day (sampling time is ∼2–12 h), which corresponds to ∼10–400 km on a spatial scale. Air temperature and relative humidity were measured at 15 m altitude on the ship. Unfortunately, reliable data of wind speed at the sampling height was not available.

[11] Figure 3 shows a vapor sampling system that was installed in the bridge deck, in the wheelhouse. The inlet of the air-sampling device, which was covered using a droplet-shielding filter, was installed on the ship at 15 m altitude. We add a bypass line to avoid ship exhaust gas contamination. The solenoid valves, which are controlled by an anemometer, were changed automatically so that the polluted air from
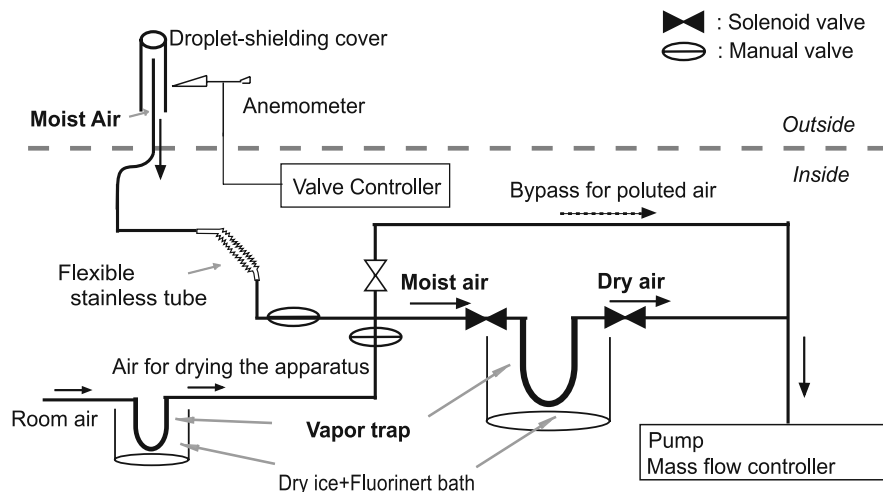

Figure 3. Schematic of the sampling system installed on the ship.

Table 2. Isotope Ratios in Water Vapor and Meteorological Conditions Along With the Ship Route

Sampling Start Time (UTC)	Sampling Duration (h)	Latitude[a] (°S)	Longtitude[a] (°E)	Atmospheric Pressure (hPa)	Air Temperature (°C)	SST(°C)	h(%)	Vapor Isotopes		
								$\delta^{18}O$(‰)	δD(‰)	d(‰)
Leg 1 (Cape Town to Antarctica)										
5 Jan. 0413	0142	38.91	20.11	1017	18.3	22.8	63.7	−15.71	−91.7	34.0
5 Jan. 0845	0300	39.86	20.53	1018	19.4	21.5	57.0	−14.56	−86.5	30.0
5 Jan. 1310	0308	40.56	20.93	1016	18.7	21.2	65.8	−14.47	−96.3	19.5
5 Jan. 1757	1056	42.59	21.75	1012	13.0	11.6	86.3	−12.09	−90.1	6.6
6 Jan. 0748	0802	45.49	22.73	989	10.8	8.2	89.3	−12.36	−96.4	2.5
6 Jan. 1740	1116	46.65	22.94	984	4.7	5.7	81.1	−15.86	−116.3	10.6
7 Jan. 0820	0440	47.45	23.05	1001	4.9	5.8	69.8	−15.93	−117.1	10.3
7 Jan. 1610	1233	49.92	24.65	999	2.4	3.7	80.1	−15.42	−115.6	7.7
8 Jan. 0810	0735	52.88	26.04	998	1.7	1.6	82.3	−13.90	−110.5	0.7
8 Jan. 1840	1020	55.51	27.17	999	0.9	1.7	71.8	−17.73	−131.6	10.2
9 Jan. 0805	0715	58.09	28.83	995	0.9	1.3	78.8	−15.87	−122.1	4.9
9 Jan. 1835	0950	60.64	30.37	996	0.3	1.1	84.4	−15.45	−123.3	0.3
10 Jan. 0800	0645	63.40	32.00	998	0.7	1.2	81.2	−16.12	−124.6	4.4
Leg 2 (Antarctic Coastal Area)										
10 Jan. 1745	0840	65.10	33.75	995	−0.3	0.0	80.1	−17.17	−134.0	3.4
11 Jan. 0610	0435	65.32	34.54	994	−0.3	0.1	79.7	−17.24	−132.2	5.8
11 Jan. 1145	0200	65.46	34.55	994	−1.6	0.1	80.7	−19.27	−150.5	3.6
11 Jan. 1502	0228	65.45	34.40	994	−1.7	0.1	84.3	−21.79	−163.3	11.1
11 Jan. 1845	0152	65.44	34.34	994	−1.9	0.2	82.6	−22.32	−169.0	9.6
11 Jan. 2218	0337	65.71	35.03	994	−1.5	−0.1	76.5	−23.94	−182.8	8.7
12 Jan. 0305	0218	66.17	35.94	993	−2.1	0.2	79.7	−24.97	−187.1	12.7
12 Jan. 0710	0805	66.17	36.15	994	−1.0	0.4	78.8	−22.15	−168.1	9.0
12 Jan. 1705	1030	65.74	36.11	997	−1.3	0.4	79.5	−22.98	−170.2	13.6
13 Jan. 0652	0828	65.15	36.05	997	0.9	1.0	84.0	−16.92	−130.2	5.1
13 Jan. 1703	0857	65.12	35.32	995	0.2	0.6	94.6	−13.57	−113.6	−5.0
14 Jan. 0740	0738	65.02	37.89	992	1.4	1.6	93.4	−15.46	−126.8	−3.1
14 Jan. 1845	0901	65.33	38.00	984	0.5	1.7	96.9	−14.58	−120.1	−3.4
15 Jan. 1300	0220	66.83	37.76	971	−0.5	0.1	95.7	−17.58	−139.2	1.5
15 Jan. 1655	1013	66.82	37.71	971	−0.5	0.0	95.1	−15.87	−128.1	−1.1
16 Jan. 0655	0755	66.59	39.01	977	−0.1	0.3	95.2	−13.32	−111.5	−5.0
16 Jan. 1710	1024	66.09	40.77	981	0.0	1.5	94.4	−13.82	−113.0	−2.4
17 Jan. 0621	0829	66.01	41.11	987	0.1	1.4	87.2	−15.12	−118.7	2.3
17 Jan. 1703	1157	65.48	42.88	987	−0.2	1.2	88.6	−14.88	−115.6	3.5
18 Jan. 1452	0823	65.50	49.76	987	−0.9	−0.2	75.4	−22.24	−160.0	17.9
19 Jan. 0025	0837	65.87	51.27	991	0.4	−0.1	60.2	−23.13	−174.1	10.9
19 Jan. 1015	1657	65.34	54.97	992	0.0	0.2	70.7	−18.35	−139.1	7.7
Leg 3 (Antarctica to Fremantle)										
20 Jan. 0540	0902	64.29	61.83	991	0.4	1.0	93.5	−13.27	−108.9	−2.8
21 Jan. 0440	0515	62.39	71.16	995	0.4	1.7	85.4	−15.61	−114.9	10.0
21 Jan. 1110	0650	61.51	74.27	995	0.3	1.8	77.0	−16.41	−120.9	10.4
21 Jan. 1942	0808	60.54	77.48	994	0.0	2.1	93.3	−15.54	−115.4	9.0
22 Jan. 0515	0655	59.45	80.79	994	1.8	2.6	74.1	−17.39	−124.3	14.8
22 Jan. 1333	0522	58.61	83.47	993	1.4	2.8	74.2	−16.45	−123.5	8.1
22 Jan. 2015	0713	57.78	85.53	993	1.8	3.3	73.7	−17.49	−130.1	9.8
23 Jan. 0455	0600	56.45	88.19	995	3.6	3.5	67.3	−17.86	−131.0	11.9
23 Jan. 1215	0603	55.41	90.24	998	3.4	3.5	70.9	−16.49	−122.8	9.1
23 Jan. 1940	0650	54.53	91.82	1003	4.6	3.7	69.5	−15.95	−115.0	12.6
24 Jan. 0636	0424	53.27	93.91	1006	5.8	4.4	64.4	−15.94	−116.5	11.0
24 Jan. 1655	0805	51.89	95.97	999	4.8	5.0	86.2	−14.64	−110.0	7.1
25 Jan. 0946	0409	49.60	98.94	992	6.3	5.9	91.4	−12.27	−98.7	−0.5
25 Jan. 1515	0933	48.66	100.27	998	6.2	6.0	84.1	−13.47	−105.7	2.0
26 Jan. 0320	0755	47.19	102.15	1008	7.7	7.4	78.7	−13.96	−108.9	2.8
26 Jan. 1445	0926	45.18	104.34	1013	8.8	9.8	80.8	−13.83	−107.0	3.6
27 Jan. 0255	0415	43.56	105.98	1016	10.0	10.6	83.7	−13.52	−104.4	3.7
27 Jan. 1110	0430	42.11	107.30	1020	10.4	11.8	66.1	−15.09	−109.5	11.2
27 Jan. 1700	0630	40.76	108.35	1022	10.8	12.5	63.0	−16.13	−116.6	12.5
28 Jan. 0505	0350	38.89	110.02	1024	12.5	14.6	66.4	−15.07	−106.2	14.4
28 Jan. 1025	0430	37.99	110.99	1025	13.0	15.6	61.8	−15.69	−109.3	16.2
28 Jan. 1615	0650	36.79	112.13	1024	13.8	16.2	64.2	−15.29	−105.8	16.5
29 Jan. 0030	0430	35.55	113.05	1025	15.2	16.8	58.2	−15.46	−104.7	19.0
29 Jan. 0645	0400	34.48	113.70	1023	17.2	18.6	62.3	−14.92	−100.4	19.0
29 Jan. 1210	0455	33.47	114.35	1022	17.0	19.4	67.3	−14.60	−97.9	18.9

[a]Latitude and longtitude are shown in decimal system.

a ship funnel was passed through the bypass line. Except for this modification, the apparatus and sampling protocols are the same as described in section 2.1. The inlet air was pulled through the apparatus (flow rate, 2.0 L/min). The collected vapor sample was melted; then poured into the glass bottle and sealed with a screw cap and wrapped with Parafilm. The